Water-wave scattering by a periodic array of arbitrary bodies

By MALTE A. PETER[1]†, MICHAEL H. MEYLAN[2] AND C. M. LINTON[3]

[1] Centre for Industrial Mathematics, FB 3, University of Bremen, Germany
[2]Department of Mathematics, University of Auckland, New Zealand
[3]Department of Mathematical Sciences, Loughborough University, UK
mpeter@math.uni-bremen.de; meylan@math.auckland.ac.nz; c.m.linton@lboro.ac.uk

An algebraically exact solution to the problem of linear water-wave scattering by a periodic array of scatterers is presented in which the scatterers may be of arbitrary shape. The method of solution is based on an interaction theory in which the incident wave on each body from all the other bodies in the array is expressed in the respective local cylindrical eigenfunction expansion. We show how to calculate the slowly convergent terms efficiently which arise in the formulation and how to calculate the scattered field far from the array. The application to the problem of linear acoustic scattering by cylinders with arbitrary cross-section is also discussed. Numerical calculations are presented to show that our results agree with previous calculations. We present some computations for the case of fixed, rigid and elastic floating bodies of negligible draft concentrating on presenting the amplitudes of the scattered waves as functions of the incident angle.

1. Introduction

The scattering of water waves by floating or submerged bodies is of wide practical importance in marine engineering. Although water waves are nonlinear, if the wave amplitude is sufficiently small, the problem can be well approximated by linear theory and linear wave theory remains the basis of most engineering design. It is also the standard model for many marine geophysical phenomena such as the wave forcing of ice floes.

The problem of the wave scattering by an infinite array of periodic and identical scatterers is a common model for wave scattering by a large but finite number of periodic scatterers, such as may be found in the construction of large off-shore structures. The periodic-array problem has been investigated by many authors. The infinite periodic-array problem in the context of water waves was considered by Spring & Monkmeyer (1975); Miles (1983); Linton & Evans (1993); Falcão (2002) although the mathematical techniques for handling such arrays have a much older provenance dating back to early twentieth century work on diffraction gratings, e.g. von Ignatowsky (1914). All of the methods developed were for scattering bodies that have simple cylindrical geometry. This leads to a great simplification because the solution to the scattering problem can be found by separation of variables. If we want to consider scattering by a periodic array of scatterers of arbitrary geometry we require a modification to these scattering theories.

† The major part of this work was completed during a research stay of the first author at the University of Auckland

For a finite number of bodies of arbitrary geometry in water of finite depth, an interaction theory was developed by Kagemoto & Yue (1986). This theory was based on Graf's addition theorem for Bessel functions which allows the incident wave on each body from the scattered wave due to all the other bodies to be expressed in the local cylindrical eigenfunction expansion. Kagemoto & Yue (1986) did not present a method to determine the diffraction matrices for bodies of arbitrary geometry and this was given by Goo & Yoshida (1990). The interaction theory was extended to infinite depth by Peter & Meylan (2004). In this present paper we use this interaction theory to derive a solution for the problem of a periodic array of arbitrary shaped scatterers.

The use of the interaction theory of Kagemoto & Yue (1986) for a periodic array requires us to find an efficient way to sum the slowly convergent series which arise in the formulation and to find an expression for the far field waves in terms of the amplitudes of the scattered waves from each body. The efficient computation of these kinds of slowly convergent series is due to Twersky (1961); Linton (1998) and the calculation of the far field is based on Twersky (1962).

Recently, motivated by modelling of wave scattering in the marginal ice zone (MIZ), Wang, Meylan & Porter (2005) considered the scattering of a periodic array of elastic plates in water of infinite depth. Their method was based on an integral-equation formulation using a periodic Green's function. Beside its application to problems of finite depth, the work presented here is significantly more efficient than the method of Wang *et al.* (2005), especially if multiple calculations are required for fixed types of bodies. Such multiple calculations are required by MIZ scattering models. Furthermore, confidence that the numerics are correct is one of the requirements for a successful wave scattering model. The results of Wang *et al.* provide a very strong numerical check for the numerics developed using the model presented here.

The MIZ is an interfacial region which forms at the boundary of the open and frozen ocean. It consists of vast fields of ice floes whose size is comparable to the dominant wavelength so that the MIZ strongly scatters the incoming waves. To understand wave propagation and scattering in the MIZ we need to understand the way in which large numbers of interacting ice floes scatter waves. One approach to this problem is to build up a model MIZ out of rows of periodic arrays of ice floes. A process of averaging over different arrangements will be required but from this, a kind of quasi two-dimensional model for wave scattering can be constructed. The accurate and efficient solution of the arbitrary periodic array scattering problem is the cornerstone of such a MIZ model. The standard model for an ice floe is a floating elastic plate of negligible draft (Squire *et al.* 1995). A method of solving for the wave response of a single ice floe of arbitrary geometry in water of infinite depth was presented in Meylan (2002). Furthermore, much research has been carried out on this model because of its additional application to very large floating structures such as a floating runway. Concerning this application, the current research is summarized in Kashiwagi (2000*b*); Watanabe, Utsunomiya & Wang (2004).

The paper is organized as follows. We first give a precise formulation of the problem under consideration and recall the cylindrical eigenfunction expansions of the water velocity potential. Following the ideas of general interaction theories, we then derive a system of equations for the unknown coefficients of the scattered wavefield in the eigenfunction expansion. In this system, the diffraction transfer matrix as well as some slowly convergent series appear. The far field is then determined in terms of these coefficients and we explicitly show how the diffraction transfer matrices of arbitrary bodies and the slowly convergent series appearing in the system of equations can be efficiently calculated. The application of our method to the acoustic scattering by a periodic array of cylinders with arbitrary cross-section as well as the water-wave scattering by an array of fixed, rigid and

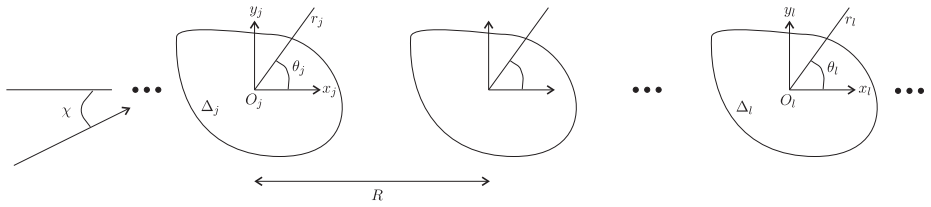

FIGURE 1. Plan view of the relation between the bodies.

flexible plates of shallow draft is discussed. Finally, we compare our results numerically to some computations from the literature and make some comparisons of arrays of fixed, rigid and flexible plates.

2. Formulation of the problem

We consider the water-wave scattering of a plane wave by an infinite array of identical vertically non-overlapping bodies, denoted by Δ_j. The mean-centre positions O_j of Δ_j are assumed to be $O_j = (jR, 0)$ where the distance between the bodies, R, is supposed sufficiently large so that there is no intersection of the smallest cylinder which contains each body, with any other body. The ambient plane wave is assumed to travel in the direction $\chi \in (0, \pi/2]$ where χ is measured with respect to the x-axis. Let (r_j, θ_j, z) be the local cylindrical coordinates of the jth body, Δ_j. Note that the zeroth body is centred at the origin and its local cylindrical coordinates coincide with the global ones, (r, θ, z). Figure 1 illustrates the setting.

The equations of motion for the water are derived from the linearized inviscid theory. Under the assumption of irrotational motion the velocity-vector field of the water can be written as the gradient field of a scalar velocity potential Φ. Assuming that the motion is time-harmonic with radian frequency ω the velocity potential can be expressed as the real part of a complex quantity,

$$\Phi(\mathbf{y}, t) = \mathrm{Re}\,\{\phi(\mathbf{y})\mathrm{e}^{-\mathrm{i}\omega t}\}. \tag{2.1}$$

To simplify notation, $\mathbf{y} = (x, y, z)$ always denotes a point in the water, which is assumed to be of constant finite depth d, while $\mathbf{x}$ always denotes a point of the undisturbed water surface assumed at $z = 0$.

Writing $\alpha = \omega^2/g$ where g is the acceleration due to gravity, the potential ϕ has to satisfy the standard boundary-value problem

$$\nabla^2\phi = 0, \qquad \mathbf{y} \in D, \tag{2.2a}$$

$$\frac{\partial\phi}{\partial z} = \alpha\phi, \qquad \mathbf{x} \in \Gamma^{\mathrm{f}}, \tag{2.2b}$$

$$\frac{\partial\phi}{\partial z} = 0, \qquad \mathbf{y} \in D,\ z = -d, \tag{2.2c}$$

where $D = (\mathbb{R}^2 \times (-d, 0))\backslash\bigcup_j \bar{\Delta}_j$ is the domain occupied by the water and Γ^{f} is the free water surface. At the immersed body surface Γ_j of Δ_j, the water velocity potential has to equal the normal velocity of the body $\mathbf{v}_j$,

$$\frac{\partial\phi}{\partial n} = \mathbf{v}_j, \qquad \mathbf{y} \in \Gamma_j. \tag{2.2d}$$

Moreover, the Sommerfeld radiation condition is imposed

$$\lim_{\tilde{r}\to\infty} \sqrt{\tilde{r}} \Big(\frac{\partial}{\partial \tilde{r}} - \mathrm{i}k \Big)(\phi - \phi^{\mathrm{In}}) = 0, \tag{2.2e}$$

where $\tilde{r}^2 = x^2 + y^2$, k is the wavenumber and ϕ^{In} is the ambient incident potential. The positive wavenumber k is related to α by the dispersion relation

$$\alpha = k \tanh kd, \tag{2.3}$$

and the values of k_m, $m > 0$, are given as positive real roots of the dispersion relation

$$\alpha + k_m \tan k_m d = 0. \tag{2.4}$$

For ease of notation, we write $k_0 = -\mathrm{i}k$. Note that k_0 is a (purely imaginary) root of (2.4).

2.1. *Eigenfunction expansion of the potential*

The scattered potential of a body Δ_j can be expanded in singular cylindrical eigenfunctions,

$$\phi_j^{\mathrm{S}}(r_j, \theta_j, z) = \sum_{m=0}^{\infty} f_m(z) \sum_{\mu=-\infty}^{\infty} A_{m\mu}^j K_\mu(k_m r_j) \mathrm{e}^{\mathrm{i}\mu\theta_j}, \tag{2.5}$$

with discrete coefficients $A_{m\mu}^j$, where

$$f_m(z) = \frac{\cos k_m(z+d)}{\cos k_m d}. \tag{2.6}$$

The incident potential upon body Δ_j can be also be expanded in regular cylindrical eigenfunctions,

$$\phi_j^{\mathrm{I}}(r_j, \theta_j, z) = \sum_{n=0}^{\infty} f_n(z) \sum_{\nu=-\infty}^{\infty} D_{n\nu}^j I_\nu(k_n r_j) \mathrm{e}^{\mathrm{i}\nu\theta_j}, \tag{2.7}$$

with discrete coefficients $D_{n\nu}^j$. In these expansions, I_ν and K_ν denote the modified Bessel functions of the first and second kind, respectively, both of order ν. Note that in (2.5) (and (2.7)) the term for $m = 0$ ($n = 0$) corresponds to the propagating modes while the terms for $m \geq 1$ ($n \geq 1$) correspond to the evanescent modes. For future reference, we remark that, for real x,

$$K_\nu(-\mathrm{i}x) = \frac{\pi \mathrm{i}^{\nu+1}}{2} H_\nu^{(1)}(x) \quad \text{and} \quad I_\nu(-\mathrm{i}x) = \mathrm{i}^{-\nu} J_\nu(x) \tag{2.8}$$

with $H_\nu^{(1)}$ and J_ν denoting the Hankel function and the Bessel function, respectively, both of first kind and order ν.

2.2. *Representation of the ambient wavefield in the eigenfunction representation*

In what follows, it is necessary to represent the ambient wavefield in the eigenfunction expansion (2.7). A short outline of how this can be accomplished is given here.

In Cartesian coordinates centred at the origin, the ambient wavefield is given by

$$\phi^{\mathrm{In}}(x, y, z) = \frac{Ag}{\omega} f_0(z) \mathrm{e}^{\mathrm{i}k(x\cos\chi + y\sin\chi)},$$

where A is the amplitude (in displacement) and χ is the angle between the x-axis and the direction in which the wavefield travels (also cf. figure 1). This expression can be

written in the eigenfunction expansion centred at the origin as

$$\phi^{\mathrm{In}}(r,\theta,z) = \frac{Ag}{\omega} f_0(z) \sum_{\nu=-\infty}^{\infty} \mathrm{e}^{\mathrm{i}\nu(\pi/2-\theta+\chi)} J_\nu(kr)$$

(Linton & McIver 2001, p. 169). The local coordinates of each body are centred at their mean-centre positions $O_l = (lR, 0)$. In order to represent the ambient wavefield, which is incident upon all bodies, in the eigenfunction expansion of an incoming wave in the local coordinates of the body, a phase factor has to be defined,

$$P_l = \mathrm{e}^{\mathrm{i}lRk\cos\chi}, \tag{2.9}$$

which accounts for the position from the origin. Including this phase factor and making use of (2.8), the ambient wavefield at the lth body is given by

$$\phi^{\mathrm{In}}(r_l,\theta_l,z) = \frac{Ag}{\omega} P_l\, f_0(z) \sum_{\nu=-\infty}^{\infty} \mathrm{e}^{\mathrm{i}\nu(\pi-\chi)} I_\nu(k_0 r_l)\mathrm{e}^{\mathrm{i}\nu\theta_l}.$$

We can therefore define the coefficients of the ambient wavefield in the eigenfunction expansion of an incident wave,

$$\tilde{D}^l_{n\nu} = \begin{cases} \frac{Ag}{\omega} P_l \mathrm{e}^{\mathrm{i}\nu(\pi-\chi)}, & n = 0, \\ 0, & n > 0. \end{cases}$$

Note that the evanescent coefficients are all zero due to the propagating nature of the ambient wave.

3. Derivation of the system of equations

Following the ideas of general interaction theories (Kagemoto & Yue 1986; Peter & Meylan 2004), a system of equations for the unknown coefficients (in the expansion (2.5)) of the scattered wavefields of all bodies is developed. This system of equations is based on transforming the scattered potential of Δ_j into an incident potential upon Δ_l ($j \neq l$). Doing this for all bodies simultaneously, and relating the incident and scattered potential for each body, a system of equations for the unknown coefficients is developed. Making use of the periodicity of the geometry and of the ambient incident wave, this system of equations can then be simplified.

The scattered potential ϕ^{S}_j of body Δ_j needs to be represented in terms of the incident potential ϕ^{I}_l upon Δ_l, $j \neq l$. From figure 1 we can see that this can be accomplished by using Graf's addition theorem for Bessel functions given in Abramowitz & Stegun (1964, eq. 9.1.79),

$$K_\tau(k_m r_j)\mathrm{e}^{\mathrm{i}\tau(\theta_j-\varphi_{j-l})} = \sum_{\nu=-\infty}^{\infty} K_{\tau+\nu}(k_m|j-l|R)\, I_\nu(k_m r_l)\mathrm{e}^{\mathrm{i}\nu(\pi-\theta_l+\varphi_{j-l})}, \quad j \neq l, \tag{3.1}$$

which is valid provided that $r_l < R$. The angles φ_n account for the difference in direction depending if the jth body is located to the left or to the right of the lth body and are defined by

$$\varphi_n = \begin{cases} \pi, & n > 0, \\ 0, & n < 0. \end{cases}$$

The limitation $r_l < R$ only requires that the escribed cylinder of each body Δ_l does not enclose any other origin O_j ($j \neq l$). However, the expansion of the scattered and

incident potential in cylindrical eigenfunctions is only valid outside the escribed cylinder of each body. Therefore the condition that the escribed cylinder of each body Δ_l does not enclose any other origin O_j $(j \neq l)$ is superseded by the more rigorous restriction that the escribed cylinder of each body may not contain any other body.

Making use of the eigenfunction expansion as well as equation (3.1), the scattered potential of Δ_j (cf. (2.5)) can be expressed in terms of the incident potential upon Δ_l as

$$\begin{aligned}
&\phi_j^{\mathrm{S}}(r_l,\theta_l,z)\\
&\quad=\sum_{m=0}^{\infty} f_m(z)\sum_{\tau=-\infty}^{\infty} A_{m\tau}^{j}\sum_{\nu=-\infty}^{\infty}(-1)^{\nu}K_{\tau-\nu}(k_m|j-l|R)I_{\nu}(k_m r_l)\mathrm{e}^{\mathrm{i}\nu\theta_l}\mathrm{e}^{\mathrm{i}(\tau-\nu)\varphi_{j-l}}\\
&\quad=\sum_{m=0}^{\infty} f_m(z)\sum_{\nu=-\infty}^{\infty}\Big[\sum_{\tau=-\infty}^{\infty} A_{m\tau}^{j}(-1)^{\nu}K_{\tau-\nu}(k_m|j-l|R)\mathrm{e}^{\mathrm{i}(\tau-\nu)\varphi_{j-l}}\Big]I_{\nu}(k_m r_l)\mathrm{e}^{\mathrm{i}\nu\theta_l}.
\end{aligned}$$

The ambient incident wavefield ϕ^{In} can also be expanded in the eigenfunctions corresponding to the incident wavefield upon Δ_l. Let $\tilde{D}_{n\nu}^{l}$ denote the coefficients of this ambient incident wavefield in the incoming eigenfunction expansion for Δ_l (cf. §2.2). The total incident wavefield upon body Δ_j can now be expressed as

$$\begin{aligned}
\phi_l^{\mathrm{I}}(r_l,\theta_l,z)&=\phi^{\mathrm{In}}(r_l,\theta_l,z)+\sum_{\substack{j=-\infty\\ j\neq l}}^{\infty}\phi_j^{\mathrm{S}}(r_l,\theta_l,z)\\
&=\sum_{n=0}^{\infty} f_n(z)\sum_{\nu=-\infty}^{\infty}\Big[\tilde{D}_{n\nu}^{l}+\sum_{\substack{j=-\infty\\ j\neq l}}^{\infty}\sum_{\tau=-\infty}^{\infty} A_{n\tau}^{j}(-1)^{\nu}K_{\tau-\nu}(k_n|j-l|R)\mathrm{e}^{\mathrm{i}(\tau-\nu)\varphi_{j-l}}\Big]\\
&\quad\times I_{\nu}(k_n r_l)\mathrm{e}^{\mathrm{i}\nu\theta_l}.
\end{aligned}$$

The coefficients of the total incident potential upon Δ_l are therefore given by

$$D_{n\nu}^{l}=\tilde{D}_{n\nu}^{l}+\sum_{\substack{j=-\infty\\ j\neq l}}^{\infty}\sum_{\tau=-\infty}^{\infty} A_{n\tau}^{j}(-1)^{\nu}K_{\tau-\nu}(k_n|j-l|R)\mathrm{e}^{\mathrm{i}(\tau-\nu)\varphi_{j-l}}. \tag{3.2}$$

In general, it is possible to relate the total incident and scattered partial waves for any body through the diffraction characteristics of that body in isolation. There exist diffraction transfer operators B^l that relate the coefficients of the incident and scattered partial waves, such that

$$A^l = B^l(D^l), \quad l \in \mathbb{Z},$$

where A^l are the scattered modes due to the incident modes D^l. Note that since it is assumed that all bodies are identical in this setting, only one diffraction transfer operator, B, is required. In the case of a countable number of modes (i.e. when the water depth is finite), B is an infinite dimensional matrix. When the modes are functions of a continuous variable (i.e. infinite depth), B is the kernel of an integral operator. The scattered and incident potential can therefore be related by a diffraction transfer operator acting in the following way,

$$A_{m\mu}^{l}=\sum_{n=0}^{\infty}\sum_{\nu=-\infty}^{\infty} B_{mn\mu\nu}D_{n\nu}^{l}. \tag{3.3}$$

If the diffraction transfer operator is known (its calculation is discussed later), the substitution of (3.2) into (3.3) gives the required equations to determine the coefficients of

the scattered wavefields of all bodies,

$$A^l_{m\mu} = \sum_{n=0}^{\infty}\sum_{\nu=-\infty}^{\infty} B_{mn\mu\nu}\Big[\tilde{D}^l_{n\nu} + \sum_{\substack{j=-\infty\\ j\neq l}}^{\infty}\sum_{\tau=-\infty}^{\infty} A^j_{n\tau}(-1)^\nu K_{\tau-\nu}(k_n|j-l|R)\mathrm{e}^{\mathrm{i}(\tau-\nu)\varphi_{j-l}}\Big], \tag{3.4}$$

$m \in \mathbb{N}$, $l, \mu \in \mathbb{Z}$.

Due to the periodicity of the geometry and of the incident wave, the coefficients $A^l_{m\mu}$ can be written as $A^l_{m\mu} = P_l A^0_{m\mu} = P_l A_{m\mu}$, say. The same can be done for the coefficients of the incident ambient wave, i.e. $\tilde{D}^l_{n\nu} = P_l \tilde{D}_{n\nu}$ (also cf. §2.2). Noting that $P_l^{-1} = P_{-l}$ and $P_j P_l = P_{j+l}$, (3.4) simplifies to

$$A_{m\mu} = \sum_{n=0}^{\infty}\sum_{\nu=-\infty}^{\infty} B_{mn\mu\nu}\Big[\tilde{D}_{n\nu} + (-1)^\nu \sum_{\tau=-\infty}^{\infty} A_{n\tau} \sum_{\substack{j=-\infty\\ j\neq l}}^{\infty} P_{j-l} K_{\tau-\nu}(k_n|j-l|R)\mathrm{e}^{\mathrm{i}(\tau-\nu)\varphi_{j-l}}\Big].$$

Introducing the constants

$$\sigma^n_\nu = \sum_{\substack{j=-\infty\\ j\neq l}}^{\infty} P_{j-l} K_\nu(k_n|j-l|R)\mathrm{e}^{\mathrm{i}\nu\varphi_{j-l}} = \sum_{j=1}^{\infty}(P_{-j} + (-1)^\nu P_j) K_\nu(k_n jR), \tag{3.5}$$

which can be evaluated separately since they do not contain any unknowns, the problem reduces to

$$A_{m\mu} = \sum_{n=0}^{\infty}\sum_{\nu=-\infty}^{\infty} B_{mn\mu\nu}\Big[\tilde{D}_{n\nu} + (-1)^\nu \sum_{\tau=-\infty}^{\infty} A_{n\tau}\, \sigma^n_{\tau-\nu}\Big]. \tag{3.6}$$

The efficient computation of the constants σ^0_ν is not trivial as the sum in (3.5) is not absolutely convergent due to the slow decay of the modified Bessel function of the second kind for large imaginary argument (The terms in the sum decay like $j^{-1/2}\mathrm{e}^{\mathrm{i}j\theta}$ for some θ). Appropriate methods for the computation of the σ^0_ν are outlined in §6. The calculation of the constants σ^n_ν, $n \neq 0$, is easy, however, since the modified Bessel function of the second kind decays exponentially for large real argument.

For numerical calculations, the infinite sums in (3.6) have to be truncated. Implying a suitable truncation, the diffraction transfer operator can be represented by a matrix $\mathbf{B}$, the finite-depth diffraction transfer matrix. Truncating the coefficients accordingly, defining $\mathbf{a}$ to be the vector of the coefficients of the scattered potential, $\mathbf{d}^{\mathrm{In}}$ to be the vector of coefficients of the ambient wavefield, and making use of the matrix $\mathbf{T}$ given by

$$(\mathbf{T})_{pq} = (-1)^q\, \sigma^n_{p-q},$$

a linear system of equations for the unknown coefficients follows from equations (3.6),

$$(\mathbf{Id} - \mathbf{B}\,{}^{\mathrm{t}}\mathbf{T})\mathbf{a} = \mathbf{B}\,\mathbf{d}^{\mathrm{In}}, \tag{3.7}$$

where the left superscript t indicates transposition and $\mathbf{Id}$ is the identity matrix of the same dimension as $\mathbf{B}$.

4. The far field

In this section, the far field is examined which describes the scattering far away from the array. The derivation is equivalent to that of Twersky (1962). First, we define the scattering angles which give the directions of propagation of plane scattered waves far

away from the array. Letting $p = 2\pi/R$, define the scattering angles χ_m by

$$\chi_m = \arccos(\psi_m/k) \quad \text{where} \quad \psi_m = k\cos\chi + mp \tag{4.1}$$

and write ψ for ψ_0. Also note that $\chi_0 = \chi$ by definition. If $|\psi_m| < k$, i.e. if

$$-1 < \cos\chi + \frac{mp}{k} < 1,$$

we say that $m \in \mathcal{M}$ and then $0 < \chi_m < \pi$. It turns out (see below) that these angles ($\pm\chi_m$ for $m \in \mathcal{M}$) are the directions in which plane waves propagate away from the array. If $|\psi_m| > k$ then χ_m is no longer real and the appropriate branch of the arccos function is given by

$$\arccos t = \begin{cases} \mathrm{i}\,\mathrm{arccosh}\, t, & t > 1, \\ \pi - \mathrm{i}\,\mathrm{arccosh}(-t) & t < -1, \end{cases}$$

with $\mathrm{arccosh}\, t = \log\left(t + \sqrt{t^2-1}\right)$ for $t > 1$.

For the total potential we have

$$\begin{aligned} \phi &= \phi^{\mathrm{In}} + \sum_{m=0}^{\infty} f_m(z) \sum_{j=-\infty}^{\infty} P_j \sum_{\mu=-\infty}^{\infty} A_{m\mu} K_\mu(k_m r_j) \mathrm{e}^{\mathrm{i}\mu\theta_j} \\ &\sim \phi^{\mathrm{In}} + \frac{\pi}{2} f_0(z) \sum_{j=-\infty}^{\infty} P_j \sum_{\mu=-\infty}^{\infty} A_{0\mu} \mathrm{i}^{\mu+1} H_\mu^{(1)}(kr_j) \mathrm{e}^{\mathrm{i}\mu\theta_j}, \end{aligned} \tag{4.2}$$

as $kr \to \infty$, away from the array axis $y = 0$, where we have used the identity (2.8).

The far field can be determined as follows. If we insert the integral representation

$$H_\mu^{(1)}(kr)\mathrm{e}^{\mathrm{i}\mu\theta} = \frac{(-\mathrm{i})^{\mu+1}}{\pi} \int_{-\infty}^{\infty} \frac{\mathrm{e}^{-k\gamma(t)|y|}}{\gamma(t)} \mathrm{e}^{\mathrm{i}kxt}\, \mathrm{e}^{\mathrm{i}\mu\,\mathrm{sgn}(y)\arccos t}\, \mathrm{d}t,$$

in which $x = r\cos\theta$, $y = r\sin\theta$ and $\gamma(t)$ is defined for real t by

$$\gamma(t) = \begin{cases} -\mathrm{i}\sqrt{1-t^2} & |t| \le 1 \\ \sqrt{t^2-1} & |t| > 1, \end{cases}$$

into (4.2) we get

$$\begin{aligned} \phi &\sim \phi^{\mathrm{In}} + \frac{1}{2} f_0(z) \sum_{\mu=-\infty}^{\infty} A_{0\mu} \sum_{j=-\infty}^{\infty} \int_{-\infty}^{\infty} \frac{\mathrm{e}^{-k\gamma(t)|y|}}{\gamma(t)} \mathrm{e}^{\mathrm{i}kxt}\, \mathrm{e}^{\mathrm{i}(\psi-kt)jR}\, \mathrm{e}^{\mathrm{i}\mu\,\mathrm{sgn}(y)\arccos t}\, \mathrm{d}t \\ &= \phi^{\mathrm{In}} + \frac{\pi}{kR} f_0(z) \sum_{\mu=-\infty}^{\infty} A_{0\mu} \sum_{j=-\infty}^{\infty} \frac{\mathrm{e}^{-k\gamma(\psi_j/k)|y|}}{\gamma(\psi_j/k)} \mathrm{e}^{\mathrm{i}x\psi_j}\, \mathrm{e}^{\mathrm{i}\mu\,\mathrm{sgn}(y)\arccos\psi_j/k} \\ &= \phi^{\mathrm{In}} + \frac{\pi\mathrm{i}}{kR} f_0(z) \sum_{\mu=-\infty}^{\infty} A_{0\mu} \sum_{j=-\infty}^{\infty} \frac{1}{\sin\chi_j} \mathrm{e}^{\mathrm{i}kr\cos(|\theta|-\chi_j)}\, \mathrm{e}^{\mathrm{i}\mu\,\mathrm{sgn}(\theta)\chi_j}, \end{aligned}$$

in which we have used the Poisson summation formula,

$$\sum_{m=-\infty}^{\infty} \int_{-\infty}^{\infty} f(u)\, \mathrm{e}^{-\mathrm{i}mu}\, \mathrm{d}u = 2\pi \sum_{m=-\infty}^{\infty} f(2m\pi).$$

The only terms which contribute to the far field are those for which $|\psi_m| < k$. Thus,

as $y \to \pm\infty$, the far field consists of a set of plane waves propagating in the directions $\theta = \pm\chi_m$:

$$\phi \sim \phi^{\mathrm{In}} + \frac{\pi \mathrm{i}}{kR} f_0(z) \sum_{m \in \mathcal{M}} \frac{1}{\sin \chi_m} \mathrm{e}^{\mathrm{i}kr\cos(\theta \mp \chi_m)} \sum_{\mu=-\infty}^{\infty} A_{0\mu}\, \mathrm{e}^{\pm \mathrm{i}\mu\chi_m}. \tag{4.3}$$

From (4.3) the amplitudes of the scattered waves for each scattering angle $\pm\chi_m$ are given in terms of the coefficients $A_{0\mu}$ by

$$A_m^{\pm} = \frac{\pi \mathrm{i}}{kR} \frac{1}{\sin \chi_m} \sum_{\mu=-\infty}^{\infty} A_{0\mu}\, \mathrm{e}^{\pm \mathrm{i}\mu\chi_m}. \tag{4.4}$$

Note that the primary reflection and transmission coefficients are recovered by A_0^- and $1 + A_0^+$, respectively.

It is implicit in all the above that $\sin \chi_m \neq 0$ for any m. If $\sin \chi_m = 0$ then we have the situation where one of the scattered plane waves propagates along the array. We will not consider this resonant case here except for stating that then, the scattered field is dominated by waves travelling along the array, either towards $x = \infty$ (if $\chi_m = 0$) or towards $x = -\infty$ (if $\chi_m = \pi$). Also, we will not consider the excitation of Rayleigh-Bloch waves, which are waves which travel along the array with a phase difference between adjacent bodies greater than Rk (cf. Porter & Evans 1999; Linton & McIver 2002, e.g.). Note that Rayleigh-Bloch waves cannot be excited in a periodic array by a plane incident wave. Both the resonant and Rayleigh-Bloch case are important but beyond the scope of the present work.

5. Calculation of the diffraction transfer matrix for bodies of arbitrary geometry

Before we can solve the systems of equations for the coefficients in the eigenfunction expansion of the scattered wavefield (3.7), we require the diffraction transfer matrix $\mathbf{B}$ which relates the incident and the scattered potential for a body Δ in isolation. The elements of the diffraction transfer matrix, $(\mathbf{B})_{pq}$, are the coefficients of the pth partial wave of the scattered potential due to a single unit-amplitude incident wave of mode q upon Δ.

An explicit method to calculate the diffraction transfer matrices for bodies of arbitrary geometry in the case of finite depth is given by Goo & Yoshida (1990). We briefly recall their results in our notation. Utilizing a Green's function the single diffraction boundary-value problem can be transformed to an integral equation for the source-strength-distribution function over the immersed surface of the body. To obtain the potential in the cylindrical eigenfunction expansion, the free-surface finite-depth Green's function given by Black (1975) and Fenton (1978),

$$G(r,\theta,z;s,\vartheta,c) = \sum_{m=0}^{\infty} N_m \cos k_m(z+d)\cos k_m(c+d) \sum_{\nu=-\infty}^{\infty} K_\nu(k_m r) I_\nu(k_m s) \mathrm{e}^{\mathrm{i}\nu(\theta-\vartheta)}, \tag{5.1}$$

is then used allowing the scattered potential to be represented in the eigenfunction expansion with the cylindrical coordinate system fixed at the point of the water surface above the mean-centre position of the body. The constants N_m are given by

$$N_m = \frac{1}{\pi} \frac{k_m^2 + \alpha^2}{d(k_m^2 + \alpha^2) - \alpha} = \frac{1}{\pi} \left(d + \frac{\sin 2k_m d}{2k_m} \right)^{-1} \tag{5.2}$$

where the latter representation is often more favourable in numerical calculations.

We assume that we have represented the scattered potential in terms of the source-strength distribution ς so that the scattered potential can be written as

$$\phi^{\mathrm{S}}(\mathbf{y}) = \int_{\Gamma} G(\mathbf{y},\zeta)\,\varsigma(\zeta)\,\mathrm{d}\sigma_\zeta, \quad \mathbf{y}\in D, \tag{5.3}$$

where D is the volume occupied by the water and Γ is the immersed surface of body Δ. The source-strength-distribution function ς can be found by solving an integral equation. The integral equation is described in Wehausen & Laitone (1960) and numerical methods for its solution are outlined in Sarpkaya & Isaacson (1981). Substituting the eigenfunction expansion of the Green's function (5.1) into (5.3), the scattered potential can be written as

$$\phi^{\mathrm{S}}(r,\theta,z) = \sum_{m=0}^{\infty} f_m(z) \sum_{\nu=-\infty}^{\infty} \left[N_m \cos^2 k_m d \int_{\Gamma} \cos k_m(c+d) I_\nu(k_m s)\mathrm{e}^{-\mathrm{i}\nu\vartheta}\varsigma(\zeta)\,\mathrm{d}\sigma_\zeta \right] \times K_\nu(k_m r)\mathrm{e}^{\mathrm{i}\nu\theta}\,\mathrm{d}\eta,$$

where $\zeta = (s,\vartheta,c)$ and $r > s$. This restriction implies that the eigenfunction expansion is only valid outside the escribed cylinder of the body.

The columns of the diffraction transfer matrix are the coefficients of the eigenfunction expansion of the scattered wavefield due to the different incident modes of unit-amplitude. The elements of the diffraction transfer matrix of a body of arbitrary shape are therefore given by

$$(\mathbf{B})_{pq} = N_m \cos^2 k_m d \int_{\Gamma} \cos k_m(c+d) I_p(k_m s)\mathrm{e}^{-\mathrm{i}p\vartheta}\varsigma_q(\zeta)\,\mathrm{d}\sigma_\zeta \tag{5.4}$$

where $\varsigma_q(\zeta)$ is the source strength distribution due to an incident potential of mode q of the form

$$\phi_q^{\mathrm{I}}(s,\vartheta,c) = f_m(c) I_q(k_m s)\mathrm{e}^{\mathrm{i}q\vartheta}. \tag{5.5}$$

It should be noted that, instead of using the source strength distribution function, it is also possible to consider an integral equation for the total potential and calculate the elements of the diffraction transfer matrix from the solution of this integral equation. An outline of this method for water of finite depth is given by Kashiwagi (2000*a*).

6. The efficient computation of the σ_ν^0

The constants σ_ν^0 (cf. (3.6)) appearing in the system of equations for the coefficients of the scattered wavefield of the bodies cannot be computed straightforwardly. This is due to the slow decay of the modified Bessel function of the second kind for large imaginary argument as was discussed in §3. First, note that

$$\sigma_\nu^0 = \sum_{j=1}^{\infty} (P_{-j} + (-1)^\nu P_j) K_\nu(-\mathrm{i}kjR) = \frac{\pi \mathrm{i}^{\nu+1}}{2} \sum_{j=1}^{\infty} (P_{-j} + (-1)^\nu P_j) H_\nu^{(1)}(kjR), \tag{6.1}$$

where we have used (2.8). Therefore, it suffices to discuss the computation of the constants $\tilde{\sigma}_\nu^0$ defined via

$$\tilde{\sigma}_\nu^0 = \sum_{j=1}^{\infty} (P_{-j} + (-1)^\nu P_j) H_\nu^{(1)}(kjR)$$

as the σ_ν^0 are then determined by $\sigma_\nu^0 = \pi/2\ \mathrm{i}^{\nu+1}\,\tilde{\sigma}_\nu^0$.

An efficient way of computing the $\tilde{\sigma}_\nu^0$ is given in Linton (1998) and the results are briefly outlined in our notation. Noting that $H_{-\nu}^{(1)}(\,\cdot\,) = (-1)^\nu H_\nu^{(1)}(\,\cdot\,)$, it suffices to discuss the computation of the σ_ν^0 for non-negative ν.

Referring to Linton (1998), the constants $\tilde{\sigma}_\nu^0$ can be written as

$$\begin{aligned}\tilde{\sigma}_0^0 = -1 - \frac{2\mathrm{i}}{\pi}\left(C + \log\frac{k}{2p}\right) + \frac{2}{Rk\sin\chi} - \frac{2\mathrm{i}(k^2+2\psi^2)}{p^3R}\zeta(3)\\ + \frac{2}{R}\sum_{m=1}^{\infty}\left(\frac{1}{k\sin\chi_{-m}} + \frac{1}{k\sin\chi_m} + \frac{2\mathrm{i}}{pm} + \frac{\mathrm{i}(k^2+2\psi^2)}{p^3m^3}\right)\end{aligned} \tag{6.2a}$$

where $C \approx 0.5772$ is Euler's constant and ζ is the Riemann zeta function and the terms in the sum converge like $O(m^{-4})$ as $m \to \infty$ (by which we mean that the summands are proportional to m^{-4} in the limit for large values of m) as well as

$$\begin{aligned}\tilde{\sigma}_{2\nu}^0 = 2(-1)^\nu\left(\frac{\mathrm{e}^{2\mathrm{i}\nu\chi}}{Rk\sin\chi} - \frac{\mathrm{i}}{\pi}\left(\frac{k}{2p}\right)^{2\nu}\zeta(2\nu+1)\right) + \frac{\mathrm{i}}{\nu\pi}\\ + 2(-1)^\nu\sum_{m=1}^{\infty}\left(\frac{\mathrm{e}^{2\mathrm{i}\nu\chi_m}}{Rk\sin\chi_m} + \frac{\mathrm{e}^{-2\mathrm{i}\nu\chi_{-m}}}{Rk\sin\chi_{-m}} + \frac{\mathrm{i}}{m\pi}\left(\frac{k}{2mp}\right)^{2\nu}\right)\\ + \frac{\mathrm{i}}{\pi}\sum_{m=1}^{\nu}\frac{(-1)^m 2^{2m}(\nu+m-1)!}{(2m)!(\nu-m)!}\left(\frac{p}{k}\right)^{2m}B_{2m}(\psi/p),\end{aligned} \tag{6.2b}$$

$$\begin{aligned}\tilde{\sigma}_{2\nu-1}^0 = -2(-1)^\nu\left(\frac{\mathrm{ie}^{\mathrm{i}(2\nu-1)\chi}}{Rk\sin\chi} - \frac{\psi R\nu}{\pi^2}\left(\frac{k}{2p}\right)^{2\nu-1}\zeta(2\nu+1)\right)\\ - 2(-1)^\nu\sum_{m=1}^{\infty}\left(\frac{\mathrm{ie}^{\mathrm{i}(2\nu-1)\chi_m}}{Rk\sin\chi_m} + \frac{\mathrm{ie}^{-\mathrm{i}(2\nu-1)\chi_{-m}}}{Rk\sin\chi_{-m}} + \frac{\psi R\nu}{m^2\pi^2}\left(\frac{k}{2mp}\right)^{2\nu-1}\right)\\ - \frac{2}{\pi}\sum_{m=0}^{\nu-1}\frac{(-1)^m 2^{2m}(\nu+m-1)!}{(2m+1)!(\nu-m-1)!}\left(\frac{p}{k}\right)^{2m+1}B_{2m+1}(\psi/p),\end{aligned} \tag{6.2c}$$

for $\nu > 0$ where B_m is the mth Bernoulli polynomial. The slowest convergence in this representation occurs in $\tilde{\sigma}_1^0$ and $\tilde{\sigma}_2^0$ in which the terms converge like $O(m^{-5})$ as $m \to \infty$.

Note that since $\sin\chi_m$ is purely imaginary for $m \notin \mathcal{M}$, the computation of the real part of $\tilde{\sigma}_{2\nu}^0$ and the imaginary part of $\tilde{\sigma}_{2\nu-1}^0$ is particularly simple. For $\nu \geq 0$, they are given by

$$\operatorname{Re}\tilde{\sigma}_{2\nu}^0 = -\delta_{\nu0} + 2(-1)^\nu\sum_{m\in\mathcal{M}}\frac{\cos 2\nu\chi_m}{Rk\sin\chi_m}, \tag{6.3a}$$

$$\operatorname{Im}\tilde{\sigma}_{2\nu+1}^0 = 2\mathrm{i}(-1)^\nu\sum_{m\in\mathcal{M}}\frac{\cos(2\nu-1)\chi_m}{Rk\sin\chi_m}, \tag{6.3b}$$

where δ_{mn} is the Kronecker delta.

7. Acoustic scattering by an infinite array of identical generalized cylinders

The theory above has so far been developed for water-wave scattering of a plane wave by an infinite array of identical arbitrary bodies. It can easily be adjusted to the (simpler)

two-dimensional problem of acoustic scattering. Namely, we consider the problem that arises when a plane sound wave is incident upon an infinite array of identical generalized cylinders (i.e. bodies which have arbitrary cross-section in the (x, y)-plane but the cross-sections at any height are identical) in an acoustic medium.

For this problem, the z-dependence can be omitted and the above theory applies with the following modifications:

(a) The dispersion relation (2.3) is replaced by $k = \omega/c$ where c is the speed of sound in the medium under consideration and the dispersion relation is (2.4) omitted.

(b) All factors $\cos k_m(z+d)$, $\cos k_m(c+d)$, $\cos k_m d$ and f_0 are replaced by 1.

(c) The factor N_0 in (5.1) is k/π.

Note that point (a) implies that there are no evanescent modes in this problem, i.e. the sums over m and n in the eigenfunction expansions (2.5) and (2.7), respectively, only contain the terms for $m = 0$ and $n = 0$. Moreover, we have $k_0 = -\mathrm{i}\,\omega/c$.

For circular cylinders, i.e. cylinders which have a circular cross-section, this problem has been considered by Linton & Evans (1993). In §9.1 we numerically compare our results for this problem with theirs.

8. Wave forcing of a fixed, rigid and flexible body of shallow draft

The theory which has been developed so far has been for arbitrary bodies. No assumption has been made about the body geometry or its equations of motion. However, we want use this theory to make calculations for the specific case of bodies of shallow draft which may be fixed (which we shall refer to as a dock), rigid, or elastic (modelled as a thin plate). In the formulation, we concentrate on the elastic case of which the other two situations are subcases. This allows us to present a range of results while focusing on the geophysical problem which motivates our work, namely the wave scattering by a field of ice floes.

8.1. *Mathematical model for an elastic plate.*

We briefly describe the mathematical model of a floating elastic plate. A more detailed account can be found in Meylan (2002); Peter & Meylan (2004). We assume that the elastic plate is sufficiently thin that we may apply the shallow-draft approximation, which essentially applies the boundary conditions underneath the plate at the water surface. Assuming the elastic plate to be in contact with the water surface at all times, its displacement W is that of the water surface and W is required to satisfy the linear plate equation in the area occupied by the elastic plate Δ. In analogy to (2.1), denoting the time-independent surface displacement (with the same radian frequency as the water velocity potential due to linearity) by w ($W = \mathrm{Re}\,\{w \exp(-\mathrm{i}\omega t)\}$), the plate equation becomes

$$D\,\nabla^4 w - \omega^2\,\rho_\Delta\,h\,w = \mathrm{i}\,\omega\,\rho\,\phi - \rho\,g\,w, \quad \mathbf{x} \in \Delta, \tag{8.1}$$

with the density of the water ρ, the modulus of rigidity of the elastic plate D, its density ρ_Δ and its thickness h. The right-hand side of (8.1) arises from the linearized Bernoulli equation. It needs to be recalled that $\mathbf{x}$ always denotes a point of the undisturbed water surface. Free-edge boundary conditions apply, namely

$$\left[\nabla^2 - (1-\nu)\left(\frac{\partial^2}{\partial s^2} + \kappa(s)\frac{\partial}{\partial n}\right)\right] w = 0, \tag{8.2}$$

$$\left[\frac{\partial}{\partial n}\nabla^2 + (1-\nu)\frac{\partial}{\partial s}\left(\frac{\partial}{\partial n}\frac{\partial}{\partial s} - \kappa(s)\frac{\partial}{\partial s}\right)\right] w = 0, \tag{8.3}$$

where ν is Poisson's ratio and

$$\nabla^2 = \frac{\partial^2}{\partial x^2} + \frac{\partial^2}{\partial y^2} = \frac{\partial^2}{\partial n^2} + \frac{\partial^2}{\partial s^2} + \kappa(s)\frac{\partial}{\partial n}. \tag{8.4}$$

Here, $\kappa(s)$ is the curvature of the boundary, $\partial\Delta$, as a function of arclength s along $\partial\Delta$; $\partial/\partial s$ and $\partial/\partial n$ represent derivatives tangential and normal to the boundary $\partial\Delta$, respectively.

Non-dimensional variables (denoted with an overbar) are introduced,

$$(\bar{x}, \bar{y}, \bar{z}) = \frac{1}{L}(x, y, z), \quad \bar{w} = \frac{w}{L}, \quad \bar{\alpha} = L\,\alpha, \quad \bar{\omega} = \omega\sqrt{\frac{L}{g}} \quad \text{and} \quad \bar{\phi} = \frac{\phi}{L\sqrt{Lg}},$$

where L is a length parameter associated with the plate. In non-dimensional variables, the equation for the elastic plate (8.1) reduces to

$$\beta\nabla^4\bar{w} - \bar{\alpha}\gamma\bar{w} = \mathrm{i}\sqrt{\bar{\alpha}}\bar{\phi} - \bar{w}, \quad \bar{\mathbf{x}} \in \bar{\Delta}, \tag{8.5}$$

with

$$\beta = \frac{D}{g\rho L^4} \quad \text{and} \quad \gamma = \frac{\rho_\Delta h}{\rho L}.$$

The constants β and γ represent the stiffness and the mass of the plate, respectively. For convenience, the overbars are dropped and non-dimensional variables are assumed in what follows.

8.2. *Method of solution*

We briefly outline our method of solution for the coupled water–elastic plate problem (details can be found in Meylan 2002). The problem for the water velocity potential is converted to an integral equation in the following way. Let G be the three-dimensional free-surface Green's function for water of finite depth. The Green's function allows the representation of the scattered water velocity potential in the standard way,

$$\phi^{\mathrm{S}}(\mathbf{y}) = \int_\Gamma \left(\phi^{\mathrm{S}}(\zeta)\,\frac{\partial G}{\partial n_\zeta}(\mathbf{y};\zeta) - G(\mathbf{y};\zeta)\,\frac{\partial \phi^{\mathrm{S}}}{\partial n_\zeta}(\zeta)\right) \mathrm{d}\sigma_\zeta, \quad \mathbf{y} \in D. \tag{8.6}$$

In the case of a shallow draft, the fact that the Green's function is symmetric and therefore satisfies the free-surface boundary condition with respect to the second variable as well can be used to simplify (8.6) drastically. Due to the linearity of the problem, the ambient incident potential can just be added to the equation to obtain the total water velocity potential, $\phi = \phi^{\mathrm{I}} + \phi^{\mathrm{S}}$. Limiting the result to the water surface leaves the integral equation for the water velocity potential under the elastic plate,

$$\phi(\mathbf{x}) = \phi^{\mathrm{I}}(\mathbf{x}) + \int_\Delta G(\mathbf{x};\xi)\big(\alpha\phi(\xi) + \mathrm{i}\sqrt{\alpha}w(\xi)\big)\,\mathrm{d}\sigma_\xi, \quad \mathbf{x} \in \Delta. \tag{8.7}$$

Since the surface displacement of the elastic plate appears in this integral equation, it is coupled with the plate equation (8.5).

8.3. *The coupled elastic plate–water equations*

Since the operator ∇^4, subject to the free-edge boundary conditions, is self-adjoint, a thin plate must possess a set of modes w^k which satisfy the free boundary conditions and the eigenvalue equation

$$\nabla^4 w^k = \lambda_k w^k.$$

The modes which correspond to different eigenvalues λ_k are orthogonal and the eigenvalues are positive and real. While the plate will always have repeated eigenvalues, orthogonal modes can still be found and the modes can be normalized. We therefore assume that the modes are orthonormal, i.e.

$$\int_{\Delta} w^j(\xi) w^k(\xi)\,\mathrm{d}\sigma_\xi = \delta_{jk}.$$

The eigenvalues λ_k have the property that $\lambda_k \to \infty$ as $k \to \infty$ and we order the modes by increasing eigenvalue. These modes can be used to expand any function over the wetted surface of the elastic plate Δ.

We expand the displacement of the plate in a finite number of modes M, i.e.

$$w(\mathbf{x}) = \sum_{k=1}^{M} c_k w^k(\mathbf{x}). \tag{8.8}$$

From the linearity of (8.7) the potential can be written in the form

$$\phi(\mathbf{x}) = \phi^0(\mathbf{x}) + \sum_{k=1}^{M} c_k \phi^k(\mathbf{x}), \tag{8.9}$$

where ϕ^0 and ϕ^k respectively satisfy the integral equations

$$\phi^0(\mathbf{x}) = \phi^{\mathrm{I}}(\mathbf{x}) + \int_{\Delta} \alpha G(\mathbf{x};\xi)\phi^0(\xi) d\sigma_\xi \tag{8.10a}$$

and

$$\phi^k(\mathbf{x}) = \int_{\Delta} G(\mathbf{x};\xi)\left(\alpha\phi^k(\xi) + \mathrm{i}\sqrt{\alpha} w^k(\xi)\right)\,\mathrm{d}\sigma_\xi. \tag{8.10b}$$

The potential ϕ^0 represents the potential due to the incoming wave assuming that the displacement of the elastic plate is zero. The potential ϕ^k represents the potential which is generated by the plate vibrating with the kth mode in the absence of any input wave forcing.

We substitute equations (8.8) and (8.9) into equation (8.5) to obtain

$$\beta \sum_{k=1}^{M} \lambda_k c_k w^k - \alpha\gamma \sum_{k=1}^{M} c_k w^k = \mathrm{i}\sqrt{\alpha}\big(\phi^0 + \sum_{k=1}^{M} c_k \phi^k\big) - \sum_{k=1}^{M} c_k w^k. \tag{8.11}$$

To solve equation (8.11) we multiply by w^j and integrate over the plate (i.e. we take the inner product with respect to w^j) taking into account the orthonormality of the modes w^j and obtain

$$\beta\lambda_k c_k + (1-\alpha\gamma)\, c_k = \int_{\Delta} \mathrm{i}\sqrt{\alpha}\big(\phi^0(\xi) + \sum_{j=1}^{N} c_j \phi^j(\xi)\big) w^k(\xi)\,\mathrm{d}\sigma_\xi, \tag{8.12}$$

which is a matrix equation in c_k.

Equation (8.12) cannot be solved without determining the modes of vibration of the thin plate w^k (along with the associated eigenvalues λ_k) and solving the integral equations (8.10). We use the finite element method to determine the modes of vibration (Zienkiewicz & Taylor 1989) and the integral equations (8.10) are solved by a constant-panel method (Sarpkaya & Isaacson 1981). The same set of nodes is used for the finite-element method and to define the panels for the integral equation.

8.4. *The fixed and rigid body cases*

The fixed and rigid body cases can easily be solved by the method outlined above since they can be considered special cases. In the problem of a fixed body (dock), the displacement is always zero, $w = 0$, so we simply need to solve equation (8.10) for $\phi = \phi^0$. For the case of a rigid body, we need to truncate the sums in (8.11) to include the first three modes only (which correspond to the three modes of rigid motion of the plate, namely the heave, pitch and roll). Note that for these modes the eigenvalue is $\lambda_k = 0$ so that the term involving the stiffness β does not appear in equation (8.12).

9. Numerical calculations

In this section, we present some numerical computations using the theory developed in the previous sections. We are particularly interested in comparisons with results from other methods as well as using our method to compare the behaviour of different bodies. Besides comparisons with results from other works, one way to check the correctness of the implementation is to verify that energy is conserved, i.e. the energy of the incoming wave must be equal to the sum of the energies of all outgoing waves. In terms of the amplitudes of the scattered waves for each scattering angle $\pm\chi_m$, $A_m^{\pm}$, (cf. (4.4)) this can be written as

$$\sin\chi = \sum_{m\in\mathcal{M}} \left(|A_m^-|^2 + |A_m^+ + \delta_{0m}|^2\right) \sin\chi_m \tag{9.1}$$

where we have assumed an ambient incident potential of unit amplitude. In all calculations presented below, the absolute value of the difference of both sides in (9.1) is at most 10^{-3}.

9.1. *Comparison with results from Linton & Evans (1993)*

We first compare our results to those of Linton & Evans (1993) who considered the acoustic scattering of a plane sound wave incident upon a periodic array of identical rigid circular cylinders of radius a. It can be noted that they also discussed the application of their theory to the water-wave scattering by an infinite row of rigid vertical circular cylinders extending throughout the water depth. Their method of solution was based on a multipole expansion but they also included a separation of variables method which can be viewed as a special case of our method.

As Linton & Evans considered circular cylinders, we need to obtain the diffraction transfer matrix of rigid circular cylinders. Due to the axisymmetry, they are particularly simple. In fact, they are diagonal with diagonal elements

$$(\mathbf{B})_{pp} = -I_p'(k_0a)/K_p'(k_0a) \tag{9.2}$$

(cf. Linton & McIver 2001, p. 177, for example). Also, there are no evanescent modes if the ambient incident wave does not contain evanescent modes (which is the case in their considerations as well as ours).

We compare Linton & Evans' results to ours in terms of the amplitudes of the scattered waves, $A_m^{\pm}$. In particular, we reproduce their figures 1 (a) and (b) (corresponding to our figure 2) which show the absolute values of the amplitudes of the scattered waves plotted against ka when $a/R = 0.2$ for the cases $\chi = \pi/2$ and $\pi/3$, respectively. Note that they use different choices for defining the incident angle and spacing of the cylinders. Since Linton & Evans only give plotted data we also plot our results (shown in figure 2). A visual comparison of the plots shows that they are in good agreement with Linton & Evans' results.

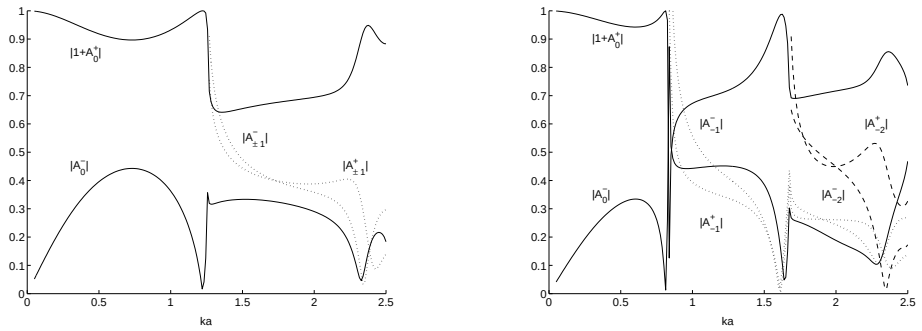

FIGURE 2. Absolute values of the amplitudes of the scattered waves plotted against ka when $a/R = 0.2$ for the two cases $\chi = \pi/2$ (left) and $\chi = \pi/3$ (right).

It is worth noting that for an ambient incident angle of $\chi = \pi/2$ (normal incidence) the scattered waves appear in pairs of two corresponding to $\pm m$, i.e. they travel in the directions $\pm\chi_m$ with respect to the array axis. Note that this is generally true for normal incidence upon arrays of arbitrary bodies and easily follows from the considerations at the beginning of §4. Moreover, as ka is increased, more scattered waves appear. From the plots in figure 2, it seems that the amplitudes of the scattered waves have poles in these points of appearance but a careful consideration shows that they are actually continuous at these points (cf. Linton & Evans 1993).

9.2. *Comparison with results from Wang* et al. *(2005)*

Next, we compare our results to those of Wang *et al.* (2005) who considered the water-wave scattering by an infinite array of floating elastic plates in water of infinite depth. The plates were modelled in exactly the same way as our elastic plates in §8. Their method of solution was based on the use of a special periodic Green's function in (8.7). As a way of testing their method, Wang *et al.* also considered the scattering from an array of docks (fixed bodies). Therefore, we reproduce their results for the dock (table 1 in Wang *et al.* 2005) and for elastic plates (table 2 in Wang *et al.* 2005) in tables 1 and 2, respectively. In both cases, the plates are of square geometry with sidelength 4 and spacing $R = 6$. The ambient wave is of the same wavelength as the sidelength of the bodies and the incident angle is $\chi = \pi/3$ (in our notation). In table 2, the elastic plates have non-dimensionalized stiffness $\beta = 0.1$ and mass $\gamma = 0$. We choose $d = 4$ in order to simulate infinite depth. Since the elastic plates tend to lengthen the wave it is necessary to choose a water depth greater than the standard choice of half the ambient wavelength (cf. Fox & Squire 1994).

As can be seen, each amplitude in table 1 has a relative difference of less than $6 \cdot 10^{-2}$ with respect to the values obtained by Wang *et al.*. The analogue is true for table 2 with a relative error of less than $9 \cdot 10^{-2}$ except for A^-_{-1} where the relative error is ≈ 0.34 (note, however, that the values in Wang *et al.* are only given up to the third decimal place). The results given in tables 1 and 2 were obtained using 23 angular propagating modes, three roots of the dispersion relation (2.4) (not counting the zeroth root) and seven corresponding angular evanescent modes each. Note that fewer modes also yield reasonably good approximations. For example, taking 15 angular propagating modes, one root of the dispersion relation and three corresponding angular evanescent modes yields answers differing from those in tables 1 and 2 only in the fourth decimal place.

m	A_m^-	A_m^+
-2	$-0.2212 - 0.0493\mathrm{i}$	$+0.2367 + 0.0268\mathrm{i}$
-1	$+0.2862 - 0.2627\mathrm{i}$	$-0.2029 + 0.3601\mathrm{i}$
0	$+0.6608 - 0.1889\mathrm{i}$	$-0.7203 - 0.1237\mathrm{i}$

TABLE 1. Amplitudes of the scattered waves for the case of a dock.

m	A_m^-	A_m^+
-2	$+0.0005 + 0.0149\mathrm{i}$	$-0.0405 - 0.0138\mathrm{i}$
-1	$-0.0202 - 0.0125\mathrm{i}$	$-0.0712 - 0.1004\mathrm{i}$
0	$-0.0627 - 0.0790\mathrm{i}$	$-0.2106 - 0.5896\mathrm{i}$

TABLE 2. Amplitudes of the scattered waves for the case of a elastic plates.

m	-5	-4	-3	-2	-1	1	2
symbol	$\circ$	$\bullet$	$\times$	$+$	$*$	$\square$	$\diamond$

TABLE 3. Symbols used to denote $|A_m^\pm|$ in the plots in figure 3.

9.3. *Comparison of the scattering by an array of docks, rigid plates and elastic plates*

In this section, we use our method to compare the behaviour of arrays of docks, rigid plates and elastic plates. The equations describing the different bodies have been derived in §8. In order to have a common setting, we choose all bodies to be square with sidelength 2 and a body spacing of $R = 4$. The ambient wavelength is $\lambda = 1.5$ and the water depth is $d = 0.5$. In figure 3, we show the absolute values of the amplitudes of the scattering waves as functions of incident angle for an array of docks, rigid plates and elastic plates, respectively. The solution of the scattering problem are shown in figure 4 for an incident angle of $\chi = \pi/5$ The elastic plates are chosen to have non-dimensional stiffness and mass $\beta = \gamma = 0.02$ while the rigid plates have the same mass. In the plots of the amplitudes of the scattered waves, we plot $|A_0^-|$ and $|1 + A_0^+|$ as solid lines and the additional scattered waves with symbols as listed in table 3. Note that the calculation of the amplitudes of the scattered waves is fairly fast since the most difficult task – the calculation of the diffraction transfer matrix – only needs to be performed once for each type of body.

From figure 3, it can be seen that docks generally reflect the energy much more than the flexible plates. From this point of view, the rigid plates can be seen as a kind of intermediate setting.

For $\chi = \pi/5 \approx 0.628$, the scattering angles are $\chi_{-4} \approx 2.33$, $\chi_{-3} \approx 1.89$, $\chi_{-2} \approx 1.51$, $\chi_{-1} \approx 1.12$ (and their negative values). The docks particularly reflect in the direction $-\chi_{-1}$ (beside $-\chi$). It can also be seen that the flexible plates already transmit most of the energy for this incident angle. The strong decrease in the amplitudes of their reflected waves appears at about $\chi \approx 0.58$. The decrease of the amplitudes of the reflected waves for the rigid plates does not appear until a larger incident angle and is also not as strong. For the docks, such a strong decrease is not observed at all. Moreover, note that all three types of bodies reflect in the direction $-\chi_1$ fairly strongly for incident angles around 0.91 (where we have $-\chi_1 \approx -0.150$ for $\chi = 0.91$).

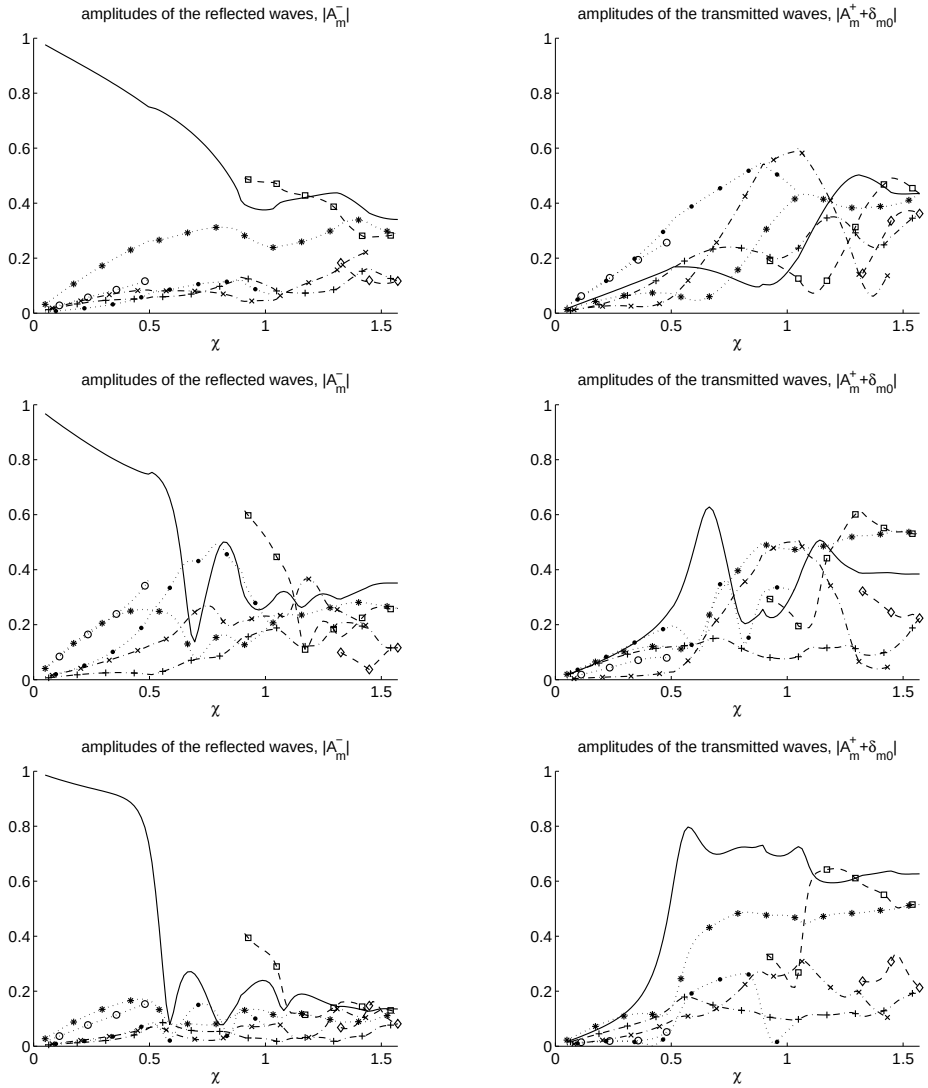

FIGURE 3. Absolute values of the amplitudes of the reflected (left) and transmitted (right) scattered waves plotted against χ. Top: docks. Middle: stiff plates ($\gamma = 0.02$). Bottom: elastic plates ($\beta = \gamma = 0.02$).

10. Summary

We have presented a solution to the problem of determining the scattering from a periodic array of scatterers of arbitrary shape. The method of solution is based on following the ideas of the interaction theory of Kagemoto & Yue (1986) and applying it to this geometry in order to obtain a system of equations in terms of the amplitudes of the scattered wavefields in the cylindrical eigenfunction expansion. We have shown how to calculate the slowly convergent series efficiently which arise in this formulation and how to determine the scattered field far from the array in terms of the amplitudes in the cylindrical eigenfunction expansion. Our numerical results agree with those presented in Linton & Evans (1993) and Wang *et al.* (2005). We have also presented results for the case of fixed, rigid and flexible arrays of bodies of negligible draft.

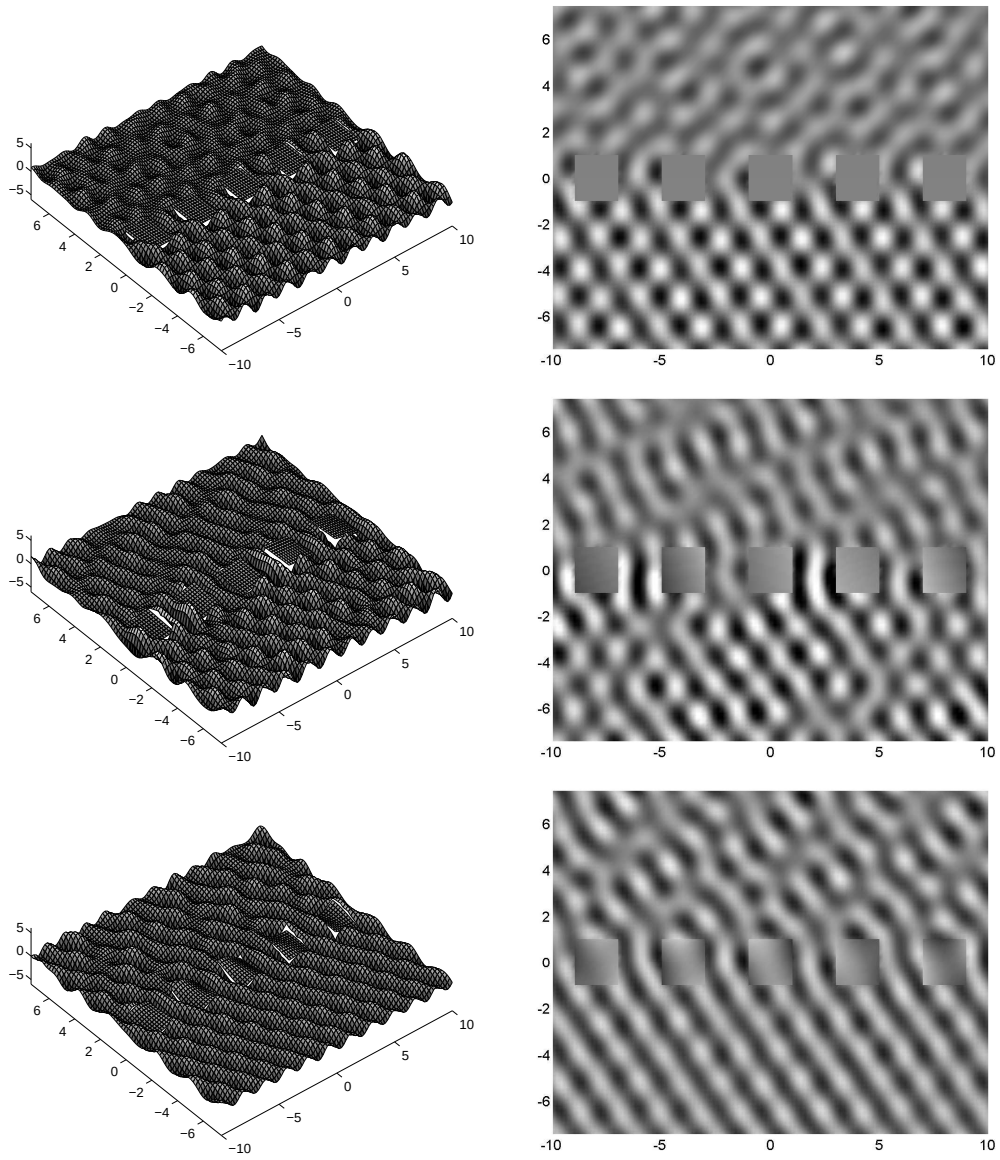

FIGURE 4. Solutions of the scattering by an array of docks (top), stiff plates (middle, $\gamma = 0.02$) and elastic plates (bottom, $\beta = \gamma = 0.02$) for an incident angle of $\chi = \pi/5$. Left: side view. Right: plan view.

This research was supported by a Marsden Grant from the New Zealand government.

REFERENCES

ABRAMOWITZ, M. & STEGUN, I., ed. 1964 *Handbook of Mathematical Functions*. Dover Inc. New York.

BLACK, J. L. 1975 Wave forces on vertical axisymmetric bodies. *J. Fluid Mech.* **67**, 369–376.

FALCÃO, A. F. D. O. 2002 Wave-power absorption by a periodic linear array of oscillating water columns. *Ocean Engineering* **29**, 1163–1186.

FENTON, J. D. 1978 Wave forces on vertical bodies of revolution. *J. Fluid Mech.* **85** (2), 241–255.

Fox, C. & Squire, V. A. 1994 On the oblique reflexion and transmission of ocean waves at shore fast sea ice. *Phil. Trans. R. Soc. Lond. A.* **347**, 185–218.

Goo, J.-S. & Yoshida, K. 1990 A numerical method for huge semisubmersible responses in waves. *SNAME Transactions* **98**, 365–387.

von Ignatowsky, W. 1914 Zur Theorie der Gitter. *Ann. Phys.* **44**, 369.

Kagemoto, H. & Yue, D. K. P. 1986 Interactions among multiple three-dimensional bodies in water waves: an exact algebraic method. *J. Fluid Mech.* **166**, 189–209.

Kashiwagi, M. 2000*a* Hydrodynamic interactions among a great number of columns supporting a very large flexible structure. *J. Fluids Struct.* **14**, 1013–1034.

Kashiwagi, M. 2000*b* Research on hydroelastic response of vlfs: Recent progress and future work. *Int. Journal of Offshore and Polar Engineering* **10** (2), 81–90.

Linton, C. M. 1998 The Green's function for the two-dimensional Helmholtz equation in periodic domains. *J. Engng. Math.* **33**, 377–402.

Linton, C. M. & Evans, D. V. 1993 The interaction of waves with a row of circular cylinders. *J. Fluid Mech.* **251**, 687–708.

Linton, C. M. & McIver, M. 2002 The existence of Rayleigh-Bloch surface waves. *J. Fluid Mech.* **470**, 85–90.

Linton, C. M. & McIver, P. 2001 *Handbook of Mathematical Techniques for Wave / Structure Interactions*. Chapman & Hall /CRC.

Meylan, M. H. 2002 Wave response of an ice floe of arbitrary geometry. *J. Geophys. Res. – Oceans* **107** (C1), doi: 10.1029/2000JC000713.

Miles, J. W. 1983 Surface-wave diffraction by a periodic row of submerged ducts. *J. Fluid Mech.* **128**, 155–180.

Peter, M. A. & Meylan, M. H. 2004 Infinite-depth interaction theory for arbitrary floating bodies applied to wave forcing of ice floes. *J. Fluid Mech.* **500**, 145–167.

Porter, R. & Evans, D. V. 1999 Rayleigh-bloch surface waves along periodic gratings and their connection with trapped modes in waveguides. *J. Fluid Mech.* **386**, 233–258.

Sarpkaya, T. & Isaacson, M. 1981 *Mechanics of Wave Forces on Offshore Structures*. Van Nostrand Reinhold.

Spring, B. H. & Monkmeyer, P. L. 1975 Interaction of plane waves with a row of cylinders. *Proc. 3rd Conf. on Civil Eng. in Oceans, ASCE* pp. 979–998.

Squire, V. A., Duggan, J. P., Wadhams, P., Rottier, P. J. & Liu, A. J. 1995 Of ocean waves and sea ice. *Annu. Rev. Fluid Mech.* **27**, 115–168.

Twersky, V. 1961 Elementary function representation of Schlömilch series. *Arch. Rational Mech. Anal.* **8**, 323–332.

Twersky, V. 1962 On scattering of waves by the infinite grating of circular cylinders. *IRE Trans. on Antennas and Propagation* **10**, 737–765.

Wang, C. D., Meylan, M. H. & Porter, R. 2005 The linear wave response of a periodic array of floating elastic plates. *J. Engng. Math.* (submitted).

Watanabe, E., Utsunomiya, T. & Wang, C. 2004 Hydroelastic analysis of pontoon-type vlfs: a literature survey. *Eng. Struct.* **26** (2), 245–256.

Wehausen, J. V. & Laitone, E. V. 1960 Surface waves. In *Fluid Dynamics III, Handbuch der Physik* (ed. S. Flügge & C. Truesdell), , vol. 9, chap. 3, pp. 446–778. Springer Verlag Berlin, also available at http://www.coe.berkeley.edu/SurfaceWaves/.

Zienkiewicz, O. C. & Taylor, R. L. 1989 *The finite element method*, 4th edn., , vol. 1. McGraw-Hill.